PREDICTED AND MEASURED VIBRATIONAL CHARACTERISTICS OF A LARGE-SCALE SHAKING TABLE FOUNDATION

H. Tajimi

SUMMARY

This paper deals with an analysis method of embedded foundations and its application to a large-scale shaking table foundation, which has recently been completed and measured for its vibrational characteristics. Typical examples are shown in comparing the precalculated and measured results. Discussions are made for flexural mode of vibration of the foundation induced by the horizontally shaking force, reduction effects of high frequency contents observed during earthquakes and evaluation of system parameters of the foundation from its seismic response.

INTRODUCTION

In 1982, a large-scale earthquake simulator facility has been completed at the Nuclear Power Engineering Test Center, which is located at Tadotsu in the western Japan. The main feature of the facility is the shaking table of 15 m x 15 m in the plane dimension. It has the capacity of subjecting test structures weighing up to 1000 tf to motions of the maximum acceleration of 1.92 g in the horizontal direction and 0.96 g in the vertical direction. The reinforced concrete mat foundation supporting the table reaction and the housing building has the rectangular plan of 90 m x 45 m with the varying depth from 21 m at the center to 13 m at the short sides, as shown in Fig. 1. The total weight of the foundation and superstructure is approximately 1.7×10^5 tf.

Prior to completion, a study group has measured systematically the vibrational characteristics of the foundation and its surrounding soil during the driving test of the shaking table in harmonic motions. The complete description of the measured results will be presented to this Conference (Ref. 1). In addition, the measurement of seismic response of the foundation and neighboring soils had started on two years ago and some records were taken during relatively small earthquakes. The author's work in the group was to precalculate the vibrational behaviors of the foundation and the surrounding soils. Owing to space limitation, this paper describes some topics to be pronounced in comparison of predicted and measured results.

METHOD OF ANALYSIS

The computational method is essentially based on a kind of the Green function method applied to a thin layered soil formation. A harmonic point load solution for the layered medium has been presented in the explicit, closed forms (Refs. 2, 3 and 4), by dealing with a thin, horizontally layered medium and assuming a linear variation of displacement across the depth of individual layer. The resulting solutions are given in Appendix for the relationships between a point load acting at the origin of the s-interface and the resulting displacements at an arbitrary point of the r-interface.

Professor of Structural Engineering, Nihon University, Tokyo, Japan

In employing the point load solution to evaluate the dynamic characteristics of an embedded foundation, it is essential to construct a three-dimensional grid of nodal points, each point lying on interfaces of layers within the soil volume to be replaced by the foundation body, as shown in Fig. 2. These nodal points serve as points, on which the concentrated forces are applied and the resulting displacements are evaluated, using the Green functions. In particular, displacements at a node just loaded should represent the displacements of the mesh stood for by the node of interest and may be approximated by the displacements at the center of a circle, whose area is equal to the mesh area associated with the node and subjected to a uniformly distributed load within it. In such a manner, the global relationship of loads and displacements at nodes within the soil block can be given by

$$\{u\} = [A(\omega)]\{P\} \tag{1}$$

where $\{u\}^T = [\{u_x\}^T \{u_y\}^T \{u_z\}^T]$, $\{P\}^T = [\{P_x\}^T \{P_y\}^T \{P_z\}^T]$.

The displacement of the soil block should be coincident with that of the foundation. The present analysis assumes that the foundation structure may be described by a flexural plate with varying rigidities in place to place. Then, the foundation motion will be expressed by superposition of translation, rocking and flexural modes. On the horizontal motion of the shaking table, the foundation is subjected to reactions of actuators which are imposed on a sidewall of the table pit. This forcing state can be divided into the symmetric and antisymmetric states, as shown in Fig. 3. The former state causes the foundation motion close to a rigid motion, while the latter produces the bending moment in the foundation structure and generates the motion in flexure, because of the actuator reactions working on the upper portion of the foundation depth.

Rigid Motion

When a foundation undergoes a rigid motion of coupled rocking and swaying, the motion can be described in terms of horizontal displacement u^x in the x-direction at the center of the foundation bottom surface and rotation angle θ^y around the central axis parallel to the y-axis, as shown in Fig. 4. Then, the nodal displacements are written by

$$\{u\} = [e^{rs}]\begin{bmatrix} u^x \\ \theta^y \end{bmatrix} \tag{2}$$

where

$$[e^{rs}] = [\{e_x\}\ \{e_\theta\}];\ \{e_x\}^T = [\{1\}^T \{0\}^T \{0\}^T],\ \{e_\theta\}^T = [\{H_j\}^T \{0\}^T \{\ell_i\}^T]$$

Substituting Eq. (2) into Eq. (1),

$$[A]^{-1}[e^{rs}]\begin{bmatrix} u^x \\ \theta^y \end{bmatrix} = \omega^2[m^*][e^{rs}]\begin{bmatrix} u^x \\ \theta^y \end{bmatrix} + \{P\} \tag{3}$$

where $[m^*] = [m^f] - [m^s]$; $[m^f]$ and $[m^s]$ denote the mass matrices of the foundation and soil block, respectively.
In the right-hand side of Eq. (3), the first term represents the nodal inertia force vector and $\{P\}$ is the external force vector. Premultiplying by $[e^{rs}]^T$, one obtains the equation of motion concerning (u^x, θ^y):

$$[e^{rs}]^T[A]^{-1}[e^{rs}]\begin{bmatrix} u^x \\ \theta^y \end{bmatrix} = \omega^2[e^{rs}]^T[m^*][e^{rs}]\begin{bmatrix} u^x \\ \theta^y \end{bmatrix} + [e^{rs}]^T\{P\} \tag{4}$$

In order to evaluate the earthquake response of foundation, it is the first step to compute the response of a soil column at the site. Then, let {g} denote the nodal displacements within the soil block developed by the soil column response. It follows that

$$[e^{rs}]^T[A]^{-1}\left([e^{rs}]\begin{bmatrix}u^x\\ \theta^y\end{bmatrix} - \{g\}\right) = \omega^2[e^{rs}]^T[m^*][e^{rs}]\begin{bmatrix}u^x\\ \theta^y\end{bmatrix} \qquad (5)$$

Flexural Motion of An Embedded Foundation

In coincidence with the possible elastic deformation of a foundation, the following displacement restrictions are required for the soil block to be replaced by the foundation:

(1) Vertical displacements at nodes along a vertical line of grid occur equally, and

(2) Horizontal displacements at nodes are neglected, because they become higher infinitesimal compared with the vertical displacements.

These conditions describes any nodes with the same plane coordinates being connected by a rigid rod vertically, as shown in Fig. 5. For this configuration, numbering the assembly of vertical rods, the stiffness matrix $[k^{zz}_{ij}]$ of soil block can be derived from Eq. (1) by putting on

$$\{u_{zj}\} = \{1\} \text{ and } \{u_{zi}\} = \{0\}, \quad i \neq j \; ; \; \{u_x\} = \{u_y\} = \{0\} \qquad (6)$$

where $\{u_{zj}\}$ denotes the vertical displacement vector for node associated with the vertical rod j. Since the stiffness matrix $[k^f_{ij}]$ of foundation can be obtained for the same nodal points by using the finite elements of flexural plate, the concerned system subjected to the external load $\{P_{zi}\}$ can be described by

$$\{P_{zi}\} = ([k^{zz}_{ij}] - [k^s_{ij}] + [k^f_{ij}] - \omega^2[m^*_j])\{u_{zj}\} \qquad (7)$$

where $[k^s_{ij}]$ denotes the stiffness matrix of the soil block which deforms in the same manner with the foundation body and $[m^*_j]$ denotes the difference of mass matrices associated with the node j of foundation and soil block.

MODELLING

The soil conditions at the site consist of deep deposit approximately 180 m thick resting on the bedrock; the upper part of the rock is weathered granite. The soil velocity was firstly measured by both seismic and borehole methods. However, the velocity of deep soils was not definite until the laboratory measurement of boring cores has been conducted. Later on the seismic observation of soil response started and the natural periods and transfer functions of horizontal motion of strata were obtained and made it possible to reexamine the profile of soil velocities. As a result, the original velocity profile was required to be revised somewhat, as presented to the Conference. But, the present analysis handles the original one, as shown in Fig. 6, because of its use for precalculation. The mathematical model of foundation and soil system was made so as to be suitable to the analysis method, as shown in Fig. 7.

VIBRATION TEST

The test was carried out by the frequency sweeping method with a table acceleration of 200 gals. At that time, the movable weight of table and other attached equipments was 650 tf, so that the driving force amplitude was 130 tf. The measured data was processed by the FFT analysis and transformed to the transfer functions, which were normalized for the shaking force of 1 tf. In Figs. 8 and 9, two examples of thus obtained resonance curves are illustrated and compared with the predicted ones.

Fig. 8 shows the resonance curves of horizontal displacement at the ground floor of the foundation structure due to the horizontally forced vibration test. It is found that both measured and predicted results are in a rough agreement. The peak at 0.8 Hz is related to the first mode of the horizontal vibration of the soil strata and the peak at 1.8 Hz is related to the coupled mode of rocking and swaying of the foundation. It was unexpected that at these peaks the measured curve was formed to be more steep.

Fig. 9 shows the resonance curves of the vertical displacement at the mid-point of the short side of the foundation due to the horizontally forced vibration. The predicted curves are drawn for two cases of rigid and flexible foundations. In the figure, it is seen that the predicted curve for the rigid foundation deviates remarkably from the measured curve for frequencies greater than 5 Hz, while the curve for the flexible foundation is close to the measured one. It is evident that the deviation in the former arose from development of symmetric flexural mode of foundation structure with such a displacement pattern as being out of phase between at the center and at the two short sides.

SEISMIC OBSERVATION

The seismic observation (Ref. 5) has pointed out the reduction effect of high frequency contents in the seismic response of the present foundation, as shown in Fig. 10. The figure indicates the spectral ratios of horizontal motions of the foundation and those at the ground surface with a distance of 100 m away from the edge of the foundation. The measured spectral ratios are given as an average for four earthquakes in the x- and y-directions and are compared with the calculated ratios. Evidently, both results are found to be in a fair agreement in each direction. The ratios gradually decrease with increase of frequency until they reach a constant. The corner frequency of 3 Hz is close to the natural frequency of soil column above the depth of the foundation bottom. Therefore, it could be understood that this reduction arose from the embedment of the foundation.

In view point of the so-called "kinematic interaction", it is instructive to evaluate the frequency response of the massless foundation concerning the present problem, when a unit harmonic motion was specified at the far ground surface. The result is shown in Fig. 11. Furthermore, the ratios of frequency responses of the foundation (in Fig. 10) to those of the massless foundation are illustrated for their top and bottom displacement in Fig. 12. Since the foundation undergoes nearly a horizontal translation in the low frequency range, these ratios are expected to be approximated by the response of a single degree of freedom system. From this consideration, it is obtained that the undamped frequency of the foundation is 2.6 Hz and the

corresponding damping ratio attains to 70 % so much.

APPENDIX

One considers the two-dimensional, time-harmonic surface waves of Rayleigh and Love types, both propagating along the x-axis in a N-1 thin layers resting on a dashpot mat which simulates a halfspace of bedrock. Then, the characteristic values of wave numbers α_k ($k = 1, 2, \ldots, 2N$) and β_k ($k = 1, 2, \ldots, N$) are determined as functions of the frequency ω for both waves respectively, to satisfy the governing equations, boundary conditions and radiation conditions of outward propagation. At the same time, the corresponding normal mode vectors are given by $\{X_k\}$ and $\{Z_k\}$ for the Rayleigh waves and $\{Y_k\}$ for the Love waves. And then, referring to the geometric relations as shown in Fig. 13, when a harmonic point load (P_x, P_y, P_z) is applied to the origin of the s-interface, the displacement (u_x, u_y, u_z) at an arbitrary point of the r-interface is obtained as

$$\begin{bmatrix} u_x \\ u_y \\ u_z \end{bmatrix} = \begin{bmatrix} V_1 \cos 2\theta + V_2 & V_1 \sin 2\theta & V_4 \cos\theta \\ V_1 \sin 2\theta & -V_1 \cos 2\theta + V_2 & V_4 \sin\theta \\ -V_3 \cos\theta & -V_3 \sin\theta & V_5 \end{bmatrix} \begin{bmatrix} P_x \\ P_y \\ P_z \end{bmatrix} \tag{8}$$

where

$$V_1 = -\frac{1}{2\pi} \sum_{k=1}^{2N} \frac{X_{rk} X_{sk}}{D_{k\alpha}} \alpha_k^2 F_1(\alpha_k r) + \frac{1}{4\pi} \sum_{k=1}^{N} \frac{Y_{rk} Y_{sk}}{D_{k\beta}} F_1(\beta_k r)$$

$$V_2 = \frac{1}{2\pi} \sum_{k=1}^{2N} \frac{X_{rk} X_{sk}}{D_{k\alpha}} \alpha_k^2 F_2(\alpha_k r) + \frac{1}{4\pi} \sum_{k=1}^{N} \frac{Y_{rk} Y_{sk}}{D_{k\beta}} F_2(\beta_k r)$$

$$V_3 = \frac{1}{\pi} \sum_{k=1}^{2N} \frac{Z_{rk} X_{sk}}{D_{k\alpha}} \alpha_k^2 F_3(\alpha_k r), \qquad V_4 = \frac{1}{\pi} \sum_{k=1}^{2N} \frac{X_{rk} Z_{sk}}{D_{k\alpha}} \alpha_k^2 F_3(\alpha_k r)$$

$$V_5 = \frac{1}{\pi} \sum_{k=1}^{2N} \frac{Z_{rk} Z_{sk}}{D_{k\alpha}} \alpha_k^2 F_2(\alpha_k r), \qquad F_1(z) = -\frac{2}{z^2} - i\frac{\pi}{2} H_2^{(2)}(z)$$

$$F_2(z) = -i\frac{\pi}{2} H_0^{(2)}(z), \qquad F_3(z) = -i\frac{\pi}{2} H_1^{(2)}(z)$$

$$D_{k\alpha} = \alpha_k^2 \{X_k\}^T [A_p] \{X_k\} + \alpha_k^2 \{Z_k\}^T [A_s] \{Z_k\} - \{X_k\}^T ([G_s] - \omega^2 [M]) \{X_k\}$$
$$- \{Z_k\}^T ([G_p] - \omega^2 [M]) \{Z_k\}$$

$D_{k\beta} = \{Y_k\}^T [A_s] \{Y_k\}$, $H_j^{(2)}(z)$ = Hankel functions of the 2nd kind,

$$[A_s]^e = GH \frac{1}{6} \begin{bmatrix} 2 & 1 \\ 1 & 2 \end{bmatrix}, \quad [G_s]^e = \frac{G}{H} \begin{bmatrix} 1 & -1 \\ -1 & 1 \end{bmatrix}, \quad [M]^e = \rho H \frac{1}{6} \begin{bmatrix} 2 & 1 \\ 1 & 2 \end{bmatrix}$$

$$[A_p]^e = (\lambda+2G) \frac{H}{6} \begin{bmatrix} 2 & 1 \\ 1 & 2 \end{bmatrix}, \quad [G_p]^e = \frac{\lambda+2G}{H} \begin{bmatrix} 1 & -1 \\ -1 & 1 \end{bmatrix}, \qquad H = \text{thickness of a layer}$$

$[A_s]$ = global matrix assembled from the element matrices $[A_s]^e$; this notation is used for other matrices.

ACKNOWLEDGEMENTS

The author wishes to thank the Committee (Chairman, Dr. M. Hayashi) of the Nuclear Power Engineering Test Center for permission to publish this study. He also thanks doctoral student M. Izumikawa for assistance.

REFERENCES

1. Research Committee of Ground Vibration (NUPEC and CRIEPI), "Experimental Project of Soil-Structure Interaction Using the Foundation of NUPEC Large Shaking Table", Proc. 8WCEE, 1984.
2. G. Waas, "Dynamisch Belastete Fundamente auf Geschichtetem Baugrund", VDI Berichte, Nr. 381, 1980, pp. 185-189.
3. H. Tajimi, "A Contribution to Theoretical Prediction of Dynamic Stiffness of Surface Foundation", Proc. 7WCEE, Vol. 5, 1980, pp. 105-112.
4. E. Kausel, "An Explicit Solution for the Green Functions for Dynamic Loads in Layered Media", Research Report R81-13, Order No. 699, Dept. of Civil Eng., M.I.T., 1981.
5. T. Sawada, et. al., "Loss Mechanism of Earthquake Motion", Proc. 6th Japan Earthquake Eng. Symposium, 1982, pp. 1553-1560.

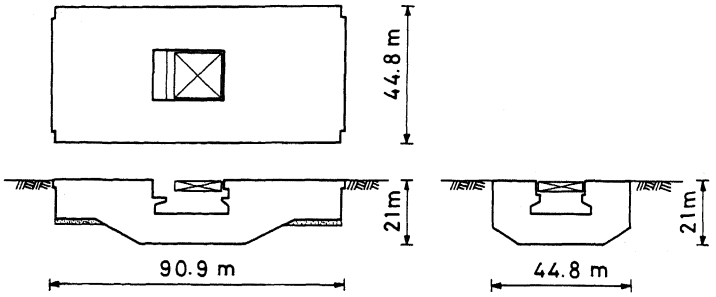

Fig. 1 Schematic section of shaking table foundation

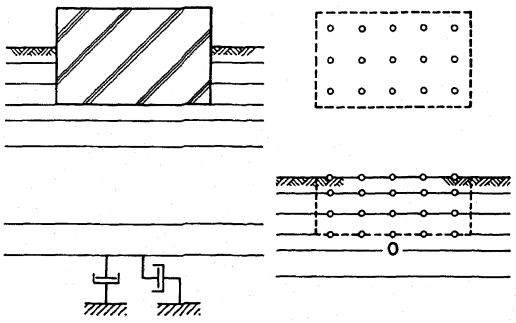

Fig. 2 Nodal assemblage of embedded foundation

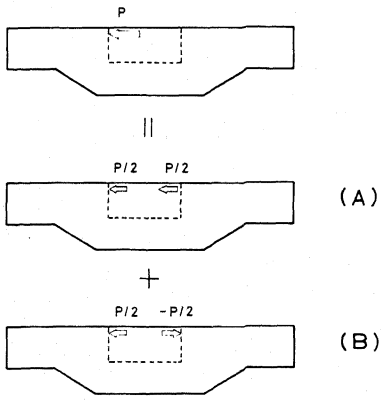

Fig. 3 Effect of horizontal actuator reaction

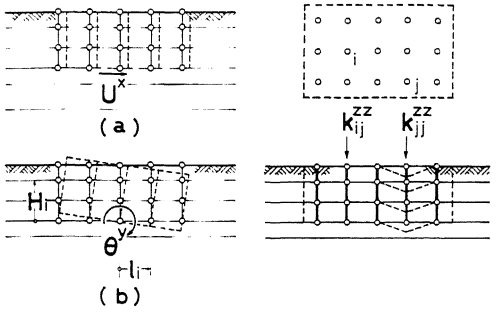

Fig. 4 Rigid motion

Fig. 5 Rigid rods representation

Depth (m)	Soil Profile	Vs (m/s)
0	Fill	160
8	Gravel -sand	200
13		320
21	Gravel -sand	360
48	Silty clay	400
78	Sand -silt	520
117	Gravel	640
181	Weathered granite	1160

Fig. 6 Soil velocity profile

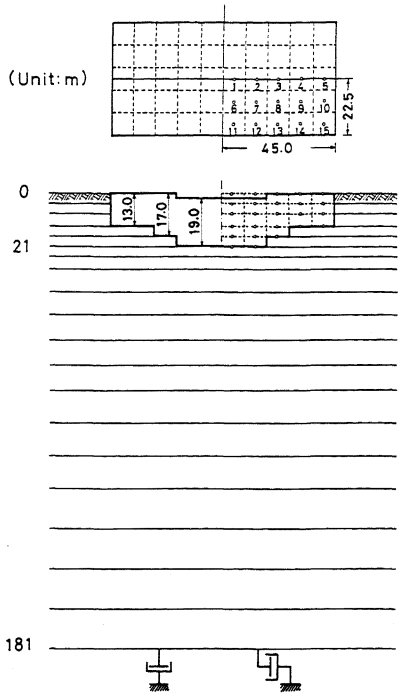

Fig. 7 Mathematical model

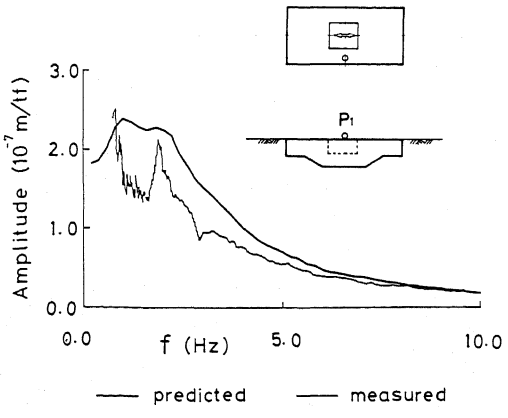

Fig. 8 Resonance curves of horizontal displacement at P_1 due to horizontal vibration of table

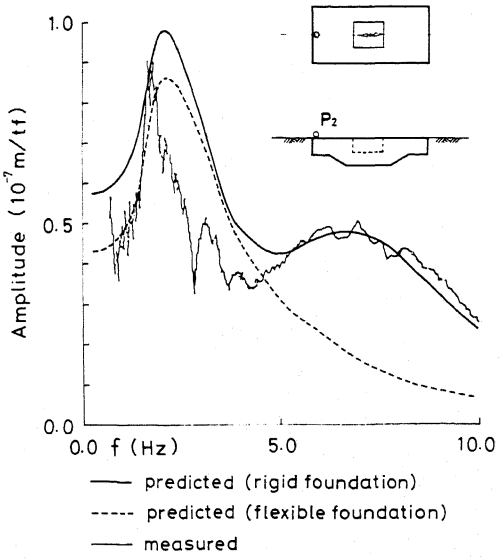

Fig. 9 Resonance curves of vertical displacement at P_2 due to horizontal vibration of table

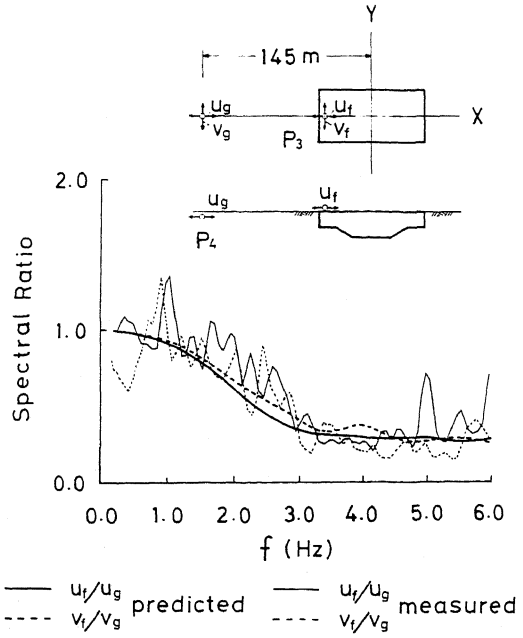

Fig. 10 Transfer functions (absolute values) of seismic response of foundation against that at free ground surface

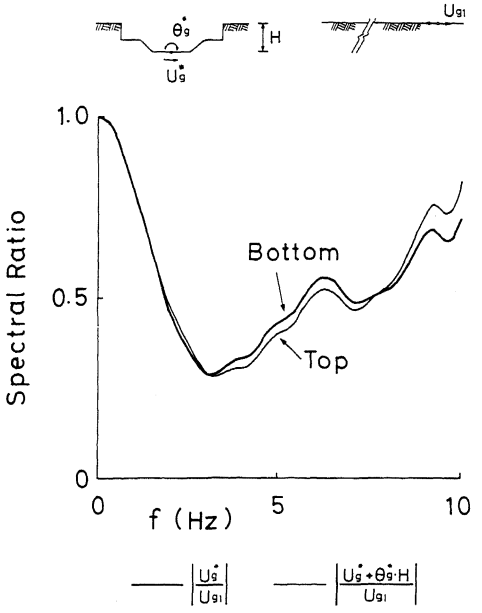

Fig. 11 Frequency response of massless foundation, when unit free surface ground motion is specified

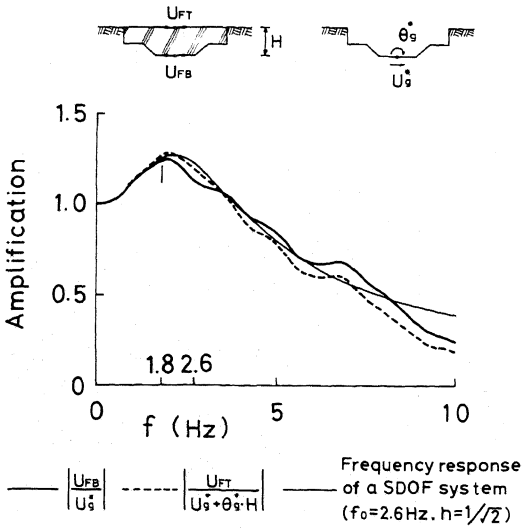

Fig. 12 Spectral ratios of foundation response to massless foundation response

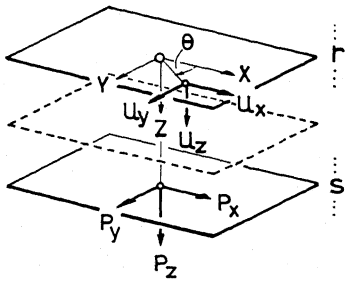

Fig. 13 Geometric relation in Eq. (8)